2015 International Conference on Unmanned Aircraft Systems (ICUAS)
Denver Marriott Tech Center
Denver, Colorado, USA, June 9-12, 2015

Short Wave Infrared (SWIR) Imaging Systems Using Small Unmanned Aerial Systems (sUAS)

Brandon Stark[1], *Student Member, IEEE*, Matthew McGee[2], *Student Member, IEEE*
and YangQuan Chen[3], *Senior Member, IEEE*

***Abstract*— Unmanned Aerial Systems are currently in use for a wide variety of applications with digital cameras and thermal cameras, but recent advances in Short Wave Infrared (SWIR) imaging systems or imagers have led to their commercial availability. The SWIR spectrum is a reflected light region and similar to near-infrared (NIR) is invisible to human eyes. The unique properties of this spectrum such as penetration of haze and smoke and its high sensitivity to moisture make it a potentially significant addition to small UAS (sUAS) applications. The use of sUASs to provide higher temporal and spatial resolutions has the potential for new applications otherwise impossible. In this paper, a tutorial introduction to the SWIR spectrum and its enabled potential applications for small UASs is presented. Furthermore this paper outlines how sUAS remote sensing applications stand to benefit from the use of SWIR imaging systems, as the effectiveness of SWIR bands in satellite imagery for metrics related to water content have already been demonstrated. Results from real world sUAS flight missions are included.**

I. Introduction

Short Wave Infrared (SWIR) imaging systems or imagers are increasingly becoming commercially available, enabling their integration into Unmanned Aerial Systems (UASs). These unique imagers measure light in the SWIR region of the electromagnetic spectrum, typically defined as between 1μm and 3μm, beyond the visible light spectrum (0.4 μm to 0.7 μm) and beyond the near infrared region (0.7 μm to 1 μm). While the near infrared (NIR) spectrum can be measured by CMOS or CCD technology even though it is invisible to the human eye, the SWIR spectrum requires a different detector, such as an Indium Gallium Arsenide (InGaAs) detector. The manufacturing challenges and costs has slowed its adoption in commercial applications. In comparison to other visible light or thermal infrared imagers, the cost for SWIR systems are typically higher and suffer from significantly reduced resolution and increased weight. However, its unique properties can provide valuable information where visible, NIR or thermal imagery are ineffective.

This paper is intended to introduce the SWIR spectrum of light, highlight some of its uses, describe its implementations and challenges including calibration techniques, demonstrate unique qualities and predict its future enabled small UAS applications. In Section II, an introduction to the SWIR spectrum is presented. Current uses of SWIR in military and remote sensing applications are described in Section III. Section IV introduces SWIR imagers and integration into UASs. Two example UAS SWIR applications are described in Section V. Finally, concluding remarks are presented in Section VI.

[1]Mechatronics, Embedded Systems and Automation Lab, School of Engineering, University of California, Merced, Merced, CA, USA, bstark2@ucmerced.edu
[2]Mechatronics, Embedded Systems and Automation Lab, School of Engineering, University of California, Merced, Merced, CA, USA, mmcgee3@ucmerced.edu
[3]Mechatronics, Embedded Systems and Automation Lab, School of Engineering, University of California, Merced, Merced, CA, USA, ychen53@ucmerced.edu

II. Short Wave Infrared

Visual light comprises of only a small portion of the electromagnetic spectrum. Beyond 0.7 μm (what humans perceive to be the color red), longer wavelengths of light exist but are invisible to the human eye. However, with the use of imaging equipment, it is possible to record these wavelengths. Many UASs are already equipped with cameras that can image in the NIR spectrum which ranges from 0.7 μm to the limit of CMOS or CCD detector sensitivity at 1 μm. Beyond NIR, from 1 μm to roughly 3 μm is referred to as the short wave infrared spectrum (Fig. 1). While this spectrum is beyond NIR, it still primarily responds to reflected electromagnetic energy as opposed to emitted energy, and thus is not normally used for thermal measurements [1]. The majority of energy in the SWIR spectrum is either reflected or absorbed by objects, similar to the light properties in the visible and NIR spectrum.

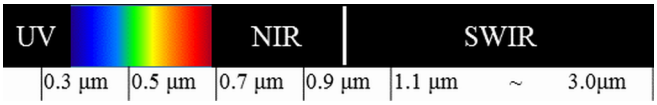

Fig. 1: Electromagnetic Light Spectrum.

The SWIR spectrum is recognized for its significant absorption by water, and bands of absorption by water vapor and CO_2. Water vapor has significant impact on the transmission of light in the atmosphere in the SWIR spectrum with bands of absorption around 0.935μm, 1.13 μm, 1.38 μm, 1.88 μm and 2.68 μm [1]. However, the strong absorption by water in the SWIR spectrum results in SWIR imagers exhibiting significant sensitivity to moisture. In Fig. 2, the water in the bottle appears dark rather than transparent. Next to the bottle, the darker spot on the apple is a visible marker of a bruise, which released moisture under the skin of the apple. In the visible spectrum, such bruising would not be visible. Man-made objects, such as clothing also typically

reflects highly in the SWIR spectrum as can be seen in Fig. 3.

Fig. 2: Water and Bruised Apple. The bruise is imperceptible in visible light, but is visible in the SWIR spectrum.

Fig. 3: Person wearing a black jacket and holding a black rock. Clothing is often highly reflective in the SWIR spectrum.

While silicon-based CCD or CMOS image sensors are unable to measure SWIR spectrum energy, silicon electroluminescence occurs in the SWIR spectrum. Applying a voltage across a silicon-based solar cell will illuminate the cells, similar to applying a voltage across an LED will illuminate the LED. This property can be used in solar cell inspection. Fig. 4a and Fig. 4b depict the difference in electroluminescence (EL) between a poorly performing solar cell (Fig. 4a) and a well-performing solar cell (Fig. 4b) as measured by a SWIR imager.

(a) EL of a poorly performing solar cell

(b) EL of a well performing solar cell

Fig. 4: Comparison of Electroluminescence of Solar Cells

III. Current SWIR Applications

The unique properties of the SWIR spectrum and SWIR imagers have led to a wide variety of applications. While there are many valuable applications in industrial processing such as solar cell inspection or art analysis, the following section will focus on existing applications where UAS integration may further enhance operation or provide additional capabilities. In this section, existing surveillance applications and remote sensing applications are introduced.

A. Surveillance

Recent advances in SWIR imagers have made them viable for military applications [2]. A comparison of visible, NIR and SWIR spectrum imagers for military applications was presented in [3]. The authors identified several potential uses where SWIR imagers have an advantage over visible and NIR cameras: haze penetration, forest and oil fire penetration, maritime and ground target contrast and long range visibility. While SWIR imagers suffer from low resolution, they are comparable to many currently available TIR imagers.

While the SWIR spectrum is a reflected spectrum, similar to visible and NIR spectrums, the longer wavelength of SWIR results in an enhanced visibility because it is less effected by the Rayleigh scattering effect. While small particles (such as in haze or smoke) scatter visible light, SWIR passes through relatively unscattered. This ability to see through haze is the key advantage for enhanced long range visibility in surveillance applications in comparison to visible light cameras. In the case of fire penetration from forest fires or oil fires, the ability of SWIR to 'see' through smoke particles has significant value.

SWIR imagers have also been shown to demonstrate a capability for low-light or night vision [4]. The high quantum efficiency of many SWIR imagers enable useful low-light operation. When combined with a SWIR illumination source, invisible to human eyes, night visibility is possible with an SWIR imager. On clear nights, the phenomenon of airglow, the faint emission of light by the atmosphere, can provide enough illumination in the SWIR spectrum to enable night time visibility for very sensitive SWIR imagers [4].

B. Satellite Imagery

Images in the SWIR spectrum are also abundant in remote sensing applications. Many satellites have imagers with

specific regions of spectral sensitivity, referred to as bands, within the SWIR region. For remote sensing applications, the SWIR spectrum is recognized for its sensitivity to moisture, which can be correlated to important metrics such as leaf water content and other crop canopy physiological statuses [5]. Over the past decades, researchers have used SWIR bands to indicate leaf and canopy moisture [6], plant water stress [7], the remote sensing of vegetation liquid water [8] and forest fire burn severity [9].

A list of common satellites and their SWIR bands can be found in Tab. I. While the majority of SWIR bands are in the region between 1.55μm and 1.75μm, some satellites have bands in the atmospheric window between 2.1μm and 2.4 μm and around 1.25μm. Landsat 8 OLI introduces a new SWIR band between 1.36-1.38μm, notable because it exists at a region where water vapor is not transparent. The result is that high altitude clouds reflect highly compared to the dark background of water vapor in the earth atmosphere, which then can be used to correct other satellite imagery distorted from these high altitude clouds.

Many of the applications utilize a common spectral vegetation difference index in the form of

$$Index = \frac{\rho_{NIR} - \rho_{SWIR}}{\rho_{NIR} + \rho_{SWIR}} \quad (1)$$

where ρ_{NIR} is the reflectance in the NIR spectrum band, ρ_{SWIR} is the reflectance in the measured SWIR spectrum. There are several indexes identified, each with different applications utilizing difference SWIR bands provided by different satellite systems. The availability of SWIR wavelengths for sUASs enable these indices to be calculated at a higher spatial resolution than previously available by utilizing optical bandpass filters. Literature describes three major spectral indices that have been identified. The Normalized Difference Water Index (NDWI) utilizes the shorter wavelengths within the SWIR spectrum (1.2 μm - 1.3 μm) and was recognized as a way to measure vegetation liquid while being less sensitive to atmospheric effects than NDVI [8]. The Normalized Difference Infrared Index (NDII) uses the SWIR spectrum between 1.55 μm - 1.75 μm and has been used to identify historic (up to 10 years) fire scar damage [10] as well as an indicator of canopy water stress [6]. The Normalized Burn Ratio (NBR) utilizes the longer SWIR spectrum between 2.05 μm - 2.45 μm to map forest burns and mapping burn severity [9].

IV. SWIR Imaging Equipment

Although not as common as digital cameras or thermal imagers, SWIR imagers have become available commercially. Currently, most SWIR imaging sensors are made with Indium Gallium Arsenide (InGaAs) detector arrays. Although other detectors such as Germanium (Ge), Indium Antimonide (InSb), and Mercury Cadmium Telluride (HgCdTe) detectors, InGeAs arrays have been more practical due to their higher quantum efficiency and low dark current at room temperature, although these sensors are typically only effective between the 0.9 μm to 1.7 μm wavelengths [4]. A plot of the quantum efficiency of an InGeAs detector can be found in Fig 5, courtesy of Infrared Cameras Inc (ICI). As with most electronics, the drive for miniaturization has led to the availability of small and light-weight systems, many suitable for integration into UASs. The rest of this section will introduce issues related to the calibration of SWIR imagers and the use of bandpass filters for SWIR spectrum separation.

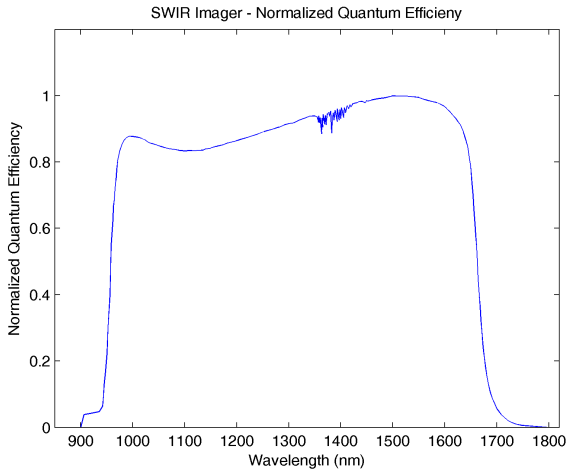

Fig. 5: SWIR Quantum Efficiency, courtesy of ICI `http://www.infraredcamerasinc.com`

A. SWIR Calibration Techniques

As with all optical imaging equipment, calibration is necessary for reliable and accurate measurements. While the SWIR spectrum is invisible to the human eye, many of the techniques of calibration for multi-spectral cameras are suitable for SWIR imagers. An in-depth discussion of many calibration techniques can be found in [11]. However, unlike visible spectrum imagers, SWIR imagers typically have a much lower resolution and pixel count which introduces additional challenges. Commercially available SWIR imagers have resolutions of 320 x 240 or 640 x 480, comparable to many commercially available TIR imagers. Special care must be taken in noise reduction techniques to prevent the obscuring of details which may result in artifacts or inaccurate data. Common issues found in SWIR imagers include pixel nonuniformities and line noise. Nonuniformity corrections (NUCs) techniques are suitable for SWIR imagers, similar to their application in thermal imagers.

In cases where reflected radiation measurements are required, radiometric calibration can be applied. Since SWIR spectrum has similar characteristics as visible and near infrared spectrums, similar radiometric calibration can be applied, however special care must be taken in target selection. Certain ink and prints may be discernible in the visible spectrum (Fig. 6a), but not in the SWIR spectrum (Fig 6b). Additionally, while SWIR is predominately a reflected energy region, objects that are extremely hot (above 300 degrees C) may emit radiation in the SWIR region and

TABLE I: Satellite SWIR Bands

Satellite	Resolution	Band Regions (μm)
ASTER	30 m	1.6-1.7, 2.145-2.185, 2.185-2.225, 2.235-2.285, 2.295-2.365, 2.360-2.430
AVHRR/3	1.09 km	1.58-1.64
EO-1 ALI	30 m	1.2-1.3, 1.55-1.75, 2.08-2.35
Landsat 7 ETM+	30 m	1.55-1.77, 2.09-2.35
Landsat 8 OLI	30 m	1.57-1.65, 2.11-2.29, 1.36-1.38
MODIS	500 m	1.23-1.25, 1.628-1.652, 2.105-2.155, 1.36-1.39

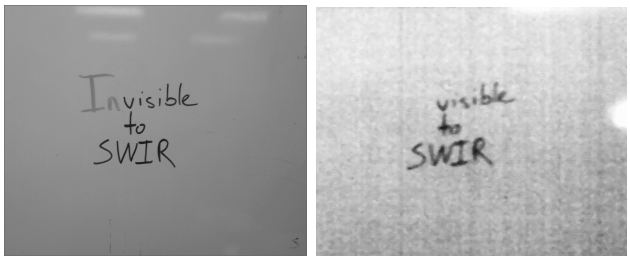

(a) Visible Spectrum (b) SWIR Spectrum

Fig. 6: Comparison of Visible and SWIR Images of marker ink. SWIR contrast artificially stretched for comparison

should be avoided for reflected energy calibration. However, once the SWIR imager is calibrated to provide accurate and repeatable data, it is suitable for surveillance applications.

B. Bandpass Lens Selection

As previously described, one application of SWIR imagers is in the field of remote sensing. It is possible to utilize bandpass optical filters to restrict wavelength sensitivity to provide similar bands as found in satellite imagery. The high quantum efficiency of InGaAs detectors enable a SWIR imager to work well in low-light situations, such as when a bandpass filter is used. This ability introduces a wide range of applications that utilize specific SWIR bands for calculation as with the previously described spectral indices that use SWIR bands. For example, a bandpass filter with a center wavelength at 1.6 μm with a bandwidth of 50 nm would result in a similar spectral sensitivity as Landsat 8 - Band 6 (1.575 μm - 1.625 μm compared to 1.570 μm to 1.650 μm).

However, there are challenges to the implementation of bandpass filters in the SWIR spectrum as there are in the visible and NIR spectrum. Many commercially available bandpass filters, including those used by many multi-spectral cameras, are subject to wavelength shifting as a function of angle of incidence. The center wavelength of a bandpass filter will shift towards towards shorter (blue) wavelengths as the viewing angle widens. This relationship can be calculated as

$$\lambda_r = \lambda_0 \left(1 - \frac{\sin^2 \theta}{n^2}\right)^{\frac{1}{2}} \tag{2}$$

where λ_r is the resulting wavelength, λ_0 is the center wavelength, n is the effective index of refraction of the filter and θ is the angle of incidence. For example, a bandpass filter centered around 1.600 μm with an index of refraction of 2.1, will have shifted to 1.580 μm when viewed at an angle of 20° (equivalent to a field of view of 40°). This may introduce significant errors for narrow bandpass filters on imagers with a wide field of view (FOV). This affect can be mitigated through the use of additional lens to collimate the light before focusing.

Bandpass filter selection should consider both the spectral reflectance of the object and the spectrum of light that passes through the atmosphere. Unlike the visible spectrum, not all sunlight passes through the atmosphere due to the bands of absorption, especially water vapor around 0.938 μm, 1.13 μm, 1.38 μm, 1.88 μm and 2.68 μm. At all of these bands, there is a limited amount of reflected energy for a SWIR to measure. This can be visualized in Fig. 7 (data reproduced from the USGS Spectral Library [12]).

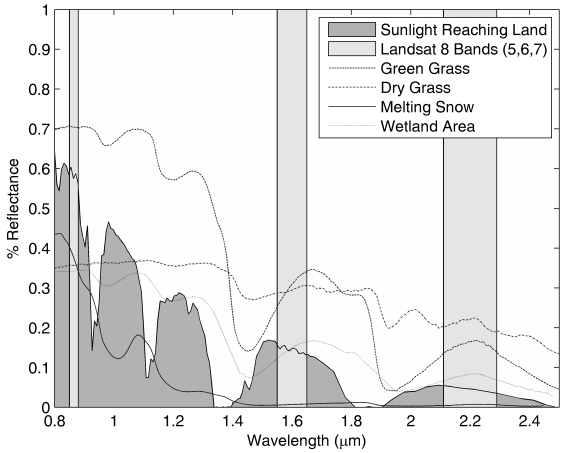

Fig. 7: Spectral Band specifications from Landsat 8, Sunlight transmission through atmosphere and spectral reflectances of green grass, dry grass, melting snow and wetland area. Spectral band specification from Landsat 8 OLI reproduced from data by [13]. Sunlight transmission data reproduced from the SMARTS model of atmospheric transfer of sunshine [14]. Spectral reflectance data reproduced from the USGS Spectral Library [12]

.

While some satellite imagery is limited by atmospheric transmission windows, a UAS with a SWIR imager with appropriate bandpass filters would be able to collect a wider range of spectral measurements. This has been shown to be valuable for improved spectral indices for water stress

detection or soil moisture measurements [15].

V. SWIR UAS Applications

The use of SWIR imagers for UAS applications is relatively unexplored and few applications have been documented. However, as SWIR imagers become more available, there will be opportunities to explore. In the following section, two specific potential applications will be discussed that highlight the unique capabilities of SWIR: soil moisture measurements and shallow vernal pool identification and analysis.

A. Soil Moisture Measurements

Recently, as much as forty-six percent of California has been classified as in stage 4 exceptional drought. As water conservation becomes ever more important in the state, agricultural regions will need to be as efficient as possible with resource allocation. To improve water conservation efforts, wide-scale water usage monitoring is necessary with sufficient spatial resolution. The use of a sUAS with a SWIR imaging system is one of the many methods proposed to provide the necessary monitoring.

Moisture effects on soil reflectance in the SWIR spectrum has been well documented with spectrometers in laboratory settings. Within the visual spectrum, wet soil reflects significantly less light than dry soil, a process that is both familiar and well studied. However, measurements of soil moisture is difficult in this range as the amount of light reflected does not vary after some level of moisture, usually within 1-2 of volumetric water content. The reflectance response to varying levels of soil moisture begins to exhibit larger separation in the NIR and SWIR range. Previous studies have identified an exponential model relating soil moisture and reflectance [16],

$$R = R_{sat} + (R_{dry} - R_{sat}) \times \exp(-c \times wc) \qquad (3)$$

where R_{sat} is the reflectance of saturated soil, R_{dry} is the reflectance of dry soil, c describes the rate of change because of soil moisture, wc is the water content (expressed as volumetric content) and all values are wavelength dependent.

This model has been validated with SWIR images as well. To validate the model, a controlled experiment was conducted. As seen in Fig. 8, 10 cups were filled with sand and mixed with distilled water. Water content was measured by volume at 2%, 5%, 8%, 11% and 15%. The set of soil samples were imaged with a SWIR imager with a full spectrum lens referred to as broadband (sensitivity between 900nm to 1700nm), a 1100nm lens with a bandwidth of 12 nm and a 1600nm lens with bandwidth of 50nm. Soil samples were intentionally not smoothed to simulate real-world conditions. Radiometric calibration was accomplished with a NIST calibrated white panel from LabSphere [17] and distilled water as the black body. Using the full spectrum of a SWIR imager (broadband) resulted in the highest nonlinearity, whereas the use of the 1600nm centered bandpass lens resulted in the most linear regression (Fig. 9). All three lens resulted in a R^2 fit to the described model above 0.9. The result of this experiment validated the use of the previously described model and validated the use of 1600 nm centered bandpass filter as the filter that would provide the most linear response to soil moisture as a function of volumetric content.

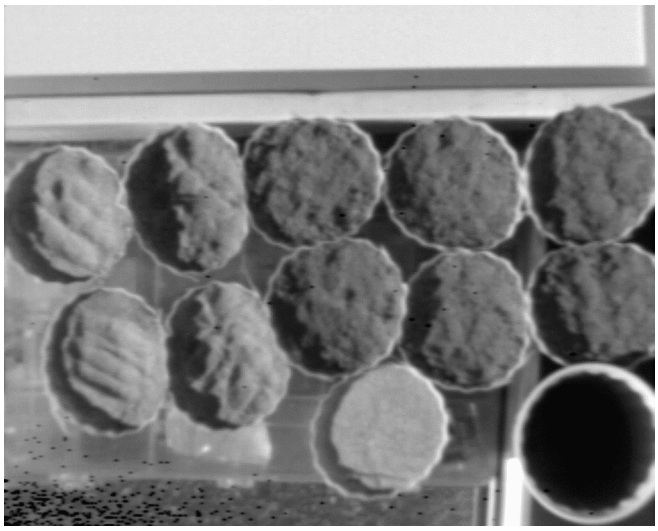

Fig. 8: Image of soil moisture data collection.

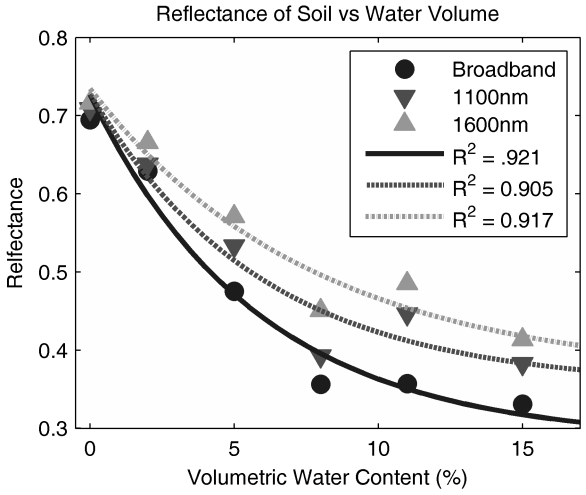

Fig. 9: Reflectance of soil as a function of water volume comparing three lens configurations. Reflectance measurements depict a more linear relationship when using a bandpass filter lens with a center wavelength at 1600nm.

Future UAS missions will combine ground truth measurements of top soil moisture with SWIR aerial imagery to validate the use of the described model for soil moisture estimation. While this application would only be effective when the soil is bare and when looking at the top layer of soil, the information would be valuable for understanding the hydrological connectivity in semi-arid environments, where many rare and endangered species of flora and fauna congregate.

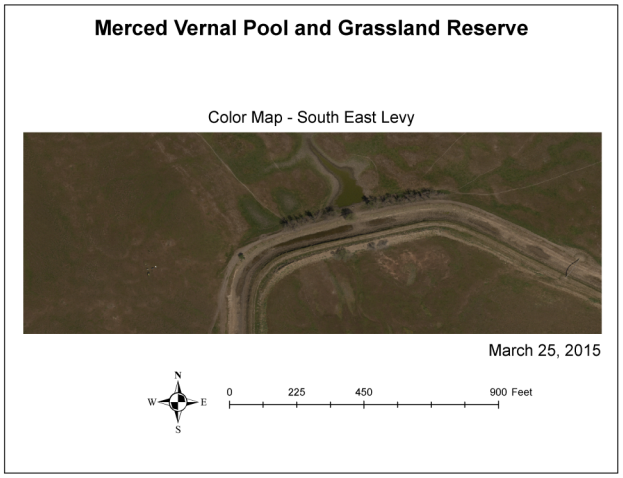

Fig. 10: Orthomap in Color

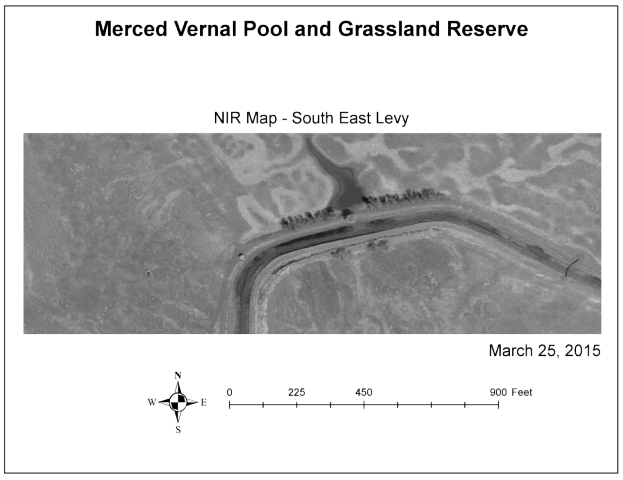

Fig. 11: Orthomap in NIR

B. Vernal Pool Identification and Analysis

In Central California, brief seasonal rain occasionally concentrates forming what is known as vernal pools. These vernal pools are critical complexes teaming with unique endemic flora and fauna. Some of these pools may only be several centimeters deep and exist for a brief week, but are a valuable ecological resource. Within Central California, the majority of the original vernal pool habitats have been destroyed through farming and urban development. Ecological monitoring and conservation of these vernal pools are critical for maintaining this part of the California ecosystem. Principally, the monitoring of ecosystem properties in these ephemeral habitats requires high frequency sensing. Traditional approaches to remote sensing, which entail fixed orbit satellites or single flight photography, fail in these systems because the identifying features are too small or too rapidly changing. The use of UASs have the potential to both provide the high spatial resolution and the high temporal resolution to both identify and quantify these vernal pools.

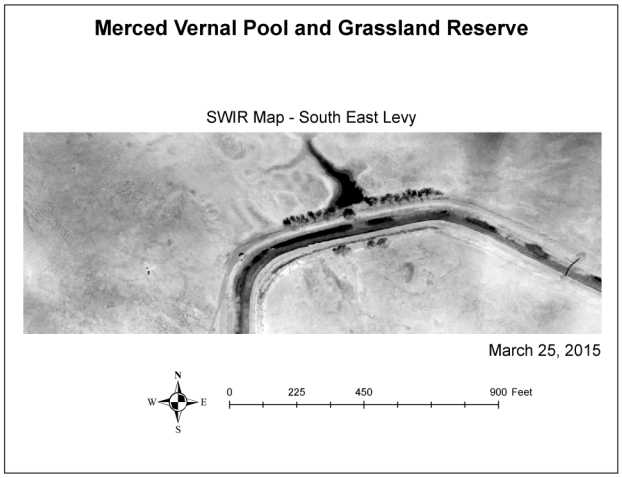

Fig. 12: Orthomap in SWIR

While NIR imagery can be used for mapping water features, energy in the NIR spectrum is not fully absorbed in water less than 1 m. An subset of sUAS imagery collected in Color, NIR, and SWIR is seen in Figures 10, 11 and 12. The shallow pool outside the levy is indistiguishable in color imagery and is faint in NIR. However, the full outline of the water level is clearly depicted in SWIR. In contrast, the deeper water pool within the levy is more apparent in NIR, however, the even more shallow ponds are indistinguishable from soil and bareground. The increased sensitivity of SWIR to water enables accurate water feature measurements which is a critical need for conservation efforts.

Future UAS missions will utilize SWIR imagery to identify and analyze the size and distribution of these temporary vernal pools to aid in the understanding and conservation of these rare and threatened ecosystems.

VI. Conclusion

SWIR imagers are starting to be become more available commercially and they hold significant potential value in providing information that would be difficult to perceive in visible, NIR or thermal imagery. When combined with the capabilities of sUASs, the possibilities are endless. The unique properties of the SWIR spectrum such as the ability to penetrate haze and smoke are extrodinarly valuable for a wide variety of surveillance, reconnaissance, or intelligence gathering for law enforcement, military or fire fighting applications. In remote sensing operations, such as agricultural or environmental applications where data analysis and processing are complex and multi-variate, SWIR reflectance measurements may prove to be key for water detection and quantification. The SWIR spectrum is already in use for these applications from satellite imagery, so the transition to sUASs is well known. The potential applications enabled through a higher spatial and temporal resolution of SWIR information are only just being realized. The validation of soil surface moisture measurements and the use of SWIR

for shallow water detection are only the beginning for SWIR applications for sUASs.

ACKNOWLEDGMENT

The authors would like to thank Gary Strahan, Abhishek Madaan and Gary Forister for their support.

REFERENCES

[1] H. G. Jones and R. A. Vaughan, *Remote Sensing of Vegetation*. Oxford University Press, New York, USA, 2010.

[2] J. Green and T. Robinson, "Test Equipment and Methods to Characterize Fully Assembled SWIR Digital Imaging Systems," in *SPIE Defense+ Security*, pp. 90710U–90710U, International Society for Optics and Photonics, 2014.

[3] R. G. Driggers, V. Hodgkin, and R. Vollmerhausen, "What good is SWIR? Passive day comparison of VIS, NIR, and SWIR," in *SPIE Defense, Security, and Sensing*, pp. 87060L–87060L, International Society for Optics and Photonics, 2013.

[4] M. P. Hansen and D. S. Malchow, "Overview of SWIR detectors, cameras, and applications," in *SPIE Defense and Security Symposium*, pp. 69390I–69390I, International Society for Optics and Photonics, 2008.

[5] D. Kimes, B. Markham, C. Tucker, and J. McMurtrey III, "Temporal relationships between spectral response and agronomic variables of a corn canopy," *Remote Sensing of Environment*, vol. 11, pp. 401–411, 1981.

[6] M. Hardisky, V. Klemas, and M. Smart, "The influence of soil salinity, growth form, and leaf moisture on the spectral radiance of *Spartina alterniflora canopies*," *Photogrammetric Engineering and Remote Sensing*, pp. 77–83, 1983.

[7] E. R. Hunt Jr and B. N. Rock, "Detection of changes in leaf water content using near-and middle-infrared reflectances," *Remote sensing of environment*, vol. 30, no. 1, pp. 43–54, 1989.

[8] B.-C. Gao, "NDWI - a normalized difference water index for remote sensing of vegetation liquid water from space," *Remote sensing of environment*, vol. 58, no. 3, pp. 257–266, 1996.

[9] C. Key and N. Benson, "Measuring and remote sensing of burn severity," in *US Geological Survey wildland fire workshop*, vol. 31, pp. 02–11, US Geological Survey Washington, DC, USA, 2002.

[10] F. Gerard, S. Plummer, R. Wadsworth, A. Ferreruela Sanfeliu, L. Iliffe, H. Balzter, and B. Wyatt, "Forest fire scar detection in the boreal forest with multitemporal SPOT-VEGETATION data," *Geoscience and Remote Sensing, IEEE Transactions on*, vol. 41, no. 11, pp. 2575–2585, 2003.

[11] J. Kelcey and A. Lucieer, "Sensor correction of a 6-band multispectral imaging sensor for UAV remote sensing," *Remote Sens*, vol. 4, no. 5, pp. 1462–1493, 2012.

[12] R. N. Clark, G. A. Swayze, R. Wise, K. E. Livo, T. M. Hoefen, R. F. Kokaly, and S. J. Sutley, *USGS digital spectral library splib06a.* US Geological Survey Reston, VA, 2007.

[13] USGS, "Landsat 8." [ONLINE] `http://landsat.usgs.gov/landsat8.php`, 2015.

[14] C. A. Gueymard, "Parameterized transmittance model for direct beam and circumsolar spectral irradiance," *Solar Energy*, vol. 71, no. 5, pp. 325–346, 2001.

[15] L. Ji, L. Zhang, B. K. Wylie, and J. Rover, "On the Terminology of the Spectral Vegetation Index (NIR- SWIR)/(NIR+ SWIR)," *International Journal of Remote Sensing*, vol. 32, no. 21, pp. 6901–6909, 2011.

[16] D. B. Lobell and G. P. Asner, "Moisture Effects on Soil Reflectance," *Soil Science Society of America Journal*, vol. 66, no. 3, pp. 722–727, 2002.

[17] Labsphere, INC, "Permaflect Reflectance Coatings." [ONLINE] `http://www.labsphere.com/products/reflectance-materials-and-coatings/white-coatings/permaflect.aspx`, 2015.